NeuroImage: Clinical 23 (2019) 101893

Contents lists available at ScienceDirect

NeuroImage: Clinical

journal homepage: www.elsevier.com/locate/ynicl

Paradoxical response inhibition advantages in adolescent obsessive compulsive disorder result from the interplay of automatic and controlled processes

Nicole Wolff*, Witold Chmielewski, Judith Buse, Veit Roessner, Christian Beste

Cognitive Neurophysiology, Department of Child and Adolescent Psychiatry, Faculty of Medicine, TU, Dresden, Germany

ARTICLE INFO

Keywords:
OCD
Response inhibition
Neurophysiology
EEG
Cognitive control

ABSTRACT

Response inhibition deficits have often been described in obsessive compulsive disorder (OCD). Yet, research on response inhibition in OCD focusses on "top-down" controlled mechanisms, and it has been neglected that response inhibition performance depends on the interplay of controlled and automatic processes during response selection. Based on pathophysiological considerations we test the counterintuitive hypothesis that OCD patients show superior inhibitory control when automatic mechanisms govern processes involved in response inhibition. We examined a group of adolescent OCD patients (n = 27) and healthy controls (n = 27) using a combined Simon-Go/NoGo task. This task is able to examine conjoint effects of automatic and controlled processes during response inhibition. EEG and source localization analyses were applied to examine the underlying neural mechanisms. OCD patients committed fewer false alarms than healthy controls (HC) in the congruent Simon-NoGo condition, which is dominated by automatic response selection mechanisms. On a neurophysiological (EEG) level, these effects were reflected by intensified correlates of 'braking' processes associated with modulation of right inferior prefrontal regions. There is no general response inhibition deficit in adolescent OCD. When considering conjoint effects of automatic and controlled processes during the inhibition of responses paradoxical response inhibition advantages can emerge in OCD. This is likely a result of otherwise pathological fronto-striatal hyperactivity and loss of a situation-specific modulation of response selection mechanisms in OCD.

1. Introduction

Obsessive compulsive disorder (OCD) is a prevalent neuropsychiatric disorder associated with unwanted mental images or urges (obsessions) as well as repetitive behaviors (compulsions) (DSM-5; APA, 2013). One major aspect that has been focused in research on OCD is 'response inhibition' (Berlin and Lee, 2018). It refers to the ability to inhibit an inappropriate response. Response inhibition is strongly deficient and a hallmark in OCD (Kang et al., 2013; Lehnen and Pietrowsky, 2015; van Velzen et al., 2014). There has been much progress in the understanding of neurofunctional correlates of these deficiencies (Kang et al., 2013). However, research on response inhibition in OCD is dominated by the view of dysfunctional "top-down" mechanisms (Berlin and Lee, 2018; Dalley et al., 2011). It has not been considered that the ability to inhibit responses is affected by at least two factors: The first factor is the degree of top-down cognitive control (Ridderinkhof et al., 2004a, 2004b; Aron, 2007). Yet, the second relevant factor is degree auf automaticity which i) affects response inhibition performance (Dippel et al., 2015; Donkers and van Boxtel, 2004) and ii) is needed to execute a pre-potent response. Importantly, controlled and automatic processes are not mutually exclusive, but exert conjoint effects during response inhibition (Chmielewski et al., 2018; Chmielewski and Beste, 2017).

Evidence for conjoint effects of automatic and controlled processes during response inhibition comes from experiments combining a "Simon Task" with a "Go/Nogo task" (Chmielewski et al., 2018; Chmielewski and Beste, 2017). In a Simon task, responses are slower and more error-prone, if the task-irrelevant stimulus location is opposed to the location of the (correct) responding effector (response button) (= incongruent trials) (Keye et al., 2013; Ridderinkhof, 2002; Wylie et al., 2010). In congruent trials, the locations of the stimulus responding effector and the (task-irrelevant) stimulus location match and responses are faster and less error-prone. Response selection in the Simon task results from a combination of automatic and controlled processes (De

* Corresponding author at: Faculty of Medicine Carl Gustav Carus, TU Dresden, Department of Child and Adolescent Psychiatry, Fetscherstrasse 74, 01307 Dresden, Germany.
E-mail address: nicole.wolff@uniklinikum-dresden.de (N. Wolff).

https://doi.org/10.1016/j.nicl.2019.101893
Received 17 January 2019; Received in revised form 4 June 2019; Accepted 6 June 2019
Available online 08 June 2019

Jong et al., 1994; Keye et al., 2013; Kornblum et al., 1990; Mückschel et al., 2016). According to the dual process account (De Jong et al., 1994), one process evokes an automatic response tendency to respond towards the location of a stimulus (="automatic" process; unconditional route). The second process is a conditional (controlled) selection of the relevant feature(s) and the appropriate response due to the stimulus-response (S-R) binding (e.g. left-pointing arrow = left button press), which requires more cognitive control (Hommel, 2011) (="controlled" process, conditional route). It has been shown that response inhibition is more difficult (error-prone), when processing is mediated via the "automatic" route (Chmielewski et al., 2018; Chmielewski and Beste, 2017). The reason is that in incongruent NoGo trials, cognitive control is exerted to overcome "automatic" processes and to resolve the conflict between the "automatic" route and the appropriate conditional selection of stimulus features. This reduces the automaticity of inappropriate response tendencies in NoGo trials and response inhibition becomes better (Chmielewski et al., 2018; Chmielewski and Beste, 2017). For congruent NoGo trials less cognitive control is employed, because the "automatic" route is in full effect and response inhibition becomes worse" (Chmielewski et al., 2018; Chmielewski and Beste, 2017). As outlined below, conjoint effects of automatic and controlled processes during response inhibition will challenge commonly held views on the nature of OCD. That means, based upon findings that cognitive and inhibitory control is diminished in OCD, it may be hypothesized that response inhibition deficits in OCD will be particularly strong when response selection depends on the "automated", compared to the "controlled" route. That is, OCD patients show a stronger impairment in congruent Simon-NoGo trials, than incongruent Simon-NoGo trials in comparison to healthy controls (HC). However, also the opposite result is possible: Differences between processes associated with the unconditional (automatic) and the conditional (controlled) route have been shown to depend on striatal mechanisms (Wylie et al., 2010; Dharmadhikari et al., 2015; Haag et al., 2015). Notably, several lines of research suggest that OCD is associated with an increased activity of striatal medium spiny neurons (MSNs) and does not show a balanced modulation of these circuits by cortical projections as evident in healthy conditions (Burguiere et al., 2015; Burguière et al., 2013). It is therefore possible that striatal neural circuits usually required during controlled (conditional) processing are overly active in OCD, regardless of whether processing depends on the "automatic", or the "controlled" route. Since OCD patients may therefore involve intensified striatal response selection mechanisms in a condition where this is likely not the case in HCs, a performance advantage may emerge. This performance advantage may then be a result of an otherwise pathological striatal hyperactivity and pathological loss of a specific modulation of response selection mechanisms. It may therefore also be hypothesized that response inhibition performance is not differentially modulated between congruent and incongruent Simon-NoGo trials in OCD patients and that there is a performance advantage in OCD patients in congruent NoGo condition, compared to HC.

In the current study we test these contradicting hypotheses on the behavioral and neurophysiological level using EEG data. Importantly, we do not focus on classical event-related potential (ERP) data. The reason is that response selection processes (codes) have been shown to be particularly relevant for conjoint effects of automatic and controlled processes during response inhibition (Chmielewski et al., 2018; Chmielewski and Beste, 2017). ERP-components are composed of various amounts of signals from different sources (Huster et al., 2015; Nunez et al., 1997; Stock et al., 2017) and also reflect a mixture of different codes related to perceptual processing ('stimulus codes') and response selection ('response selection codes') (Folstein and Van Petten, 2008). These coding levels can co-exist during the inhibition of responses (Mückschel et al., 2017) and can be dissociated using temporal signal decomposition methods (Mückschel et al., 2017b; Chmielewski et al., 2018); i.e. using residue iteration decomposition (RIDE) (Ouyang et al., 2015a, 2015b). Using RIDE, "response selection codes" have been shown to be reflected by the RIDE "C-cluster" (Bluschke et al., 2017; Mückschel et al., 2017; Ouyang et al., 2017; Verleger et al., 2014, 2017; Wolff et al., 2017), while stimulus-related codes/processes (like perception and attention) are reflected by the S-cluster (Ouyang et al., 2011, 2015a). Notably, it has been shown that only 'response selection' codes (C-cluster), but not 'stimulus codes' or a mixture of these processes reflected by ERPs, best reflect conjoint effects of "automatic" and "controlled" processes during response inhibition (Chmielewski et al., 2018). It is therefore be hypothesized that particularly the C-cluster reflects differential modulations between OCD patients and controls as a function of congruent and incongruent trial types during response inhibition. Processes reflected by the C-cluster during the inhibition of responses have been shown to be associated with the right inferior frontal gyrus (rIFG, Mückschel et al., 2017). Since the rIFG is part of the response inhibition network (Allen et al., 2018; Aron et al., 2014; Bari and Robbins, 2013; Chambers et al., 2007; Di Russo et al., 2016), we expected this region to be associated with differentially modulated conjoint effects of automatic and controlled processes during response inhibition in OCD and HC.

2. Materials and methods

2.1. Participants

Assuming a conservative effect size of f = 0.23/ 5% explained variance ($\eta_p^2 \sim 0.005$), the a-priori power calculation indicated that $N = 54$ participants ($N = 27$ OCD patients and $N = 27$ healthy controls, HC) are required to achieve a power > 95%. As shown in the results section, this estimated effect sizes matches the actually obtained effect sizes.

Patients were recruited from the outpatient clinical of the Department of Child and Adolescent Psychiatry, TU Dresden. They were recruited by telephone by presenting the study and asking if they want to participate. Healthy controls were recruited by newspaper announcements. In the OCD and HC group, $N = 16$ females were included. The intelligence quotient (IQ) of all participants was measured using the German version of the HAWIK III (Petermann and Petermann, 2010). OCD patients were 13.8 years (± 2.34) and revealed an IQ of 107.52 (± 10.70). HC were 13.93 years (± 2.05) and revealed an IQ of 110.63 ± 10.85. The groups did not differ in age, sex and IQ (all $t < 0.992$, $p > .326$). OCD patients were diagnosed by child- and adolescents psychiatrists using ICD-10 criteria (Döpfner et al., 2008). In addition to ICD-10 criteria clinical assessment tools, like "the Zwangsinventar für Kinder und Jugendliche" (ZWIK) (Goletz and Döpfner, 2011) was used. Total Score of ZWIK-Self-Scale: $M = 60.13$ (± 21.05), Total Score of the ZWIK-Parent-Scale: $M = 69.13$ (± 25.05). The German version of the Children's Yale–Brown Obsessive–Compulsive Scale (Cy-BOCS) (Foa et al., 2002) was also used; Obsessions-Score: $M = 23.26$ (± 5.05), Compulsions-Score: $M = 19.13$ (± 7.05), Total-Score: $M = 29.13$ (± 6.05). Within the OCD group, $N = 3$ patients (11%) were additionally to OCD diagnosed with a mild depressive disorder, $N = 2$ (7%) with a chronic motor or vocal tic disorder, N = 2 (7%) with social anxiety disorder of childhood, N = 1 (4%) with an adjustment disorder, N = 1 with an attention deficit hyperactivity disorder, N = 1 with a social phobia and N = 1 with an expressive language disorder. In addition, within the OCD group N = 2 patients received medication (i.e. Fluoxetin). All participants were right handed and had normal or respectively corrected to normal vision. They received an allowance of 10EUR for participation.

2.2. Task

To examine conjoint effects of 'automaticity' and 'cognitive control' during response inhibition we use a combined Simon-Go/NoGo task. The task is shown in Fig. 1.

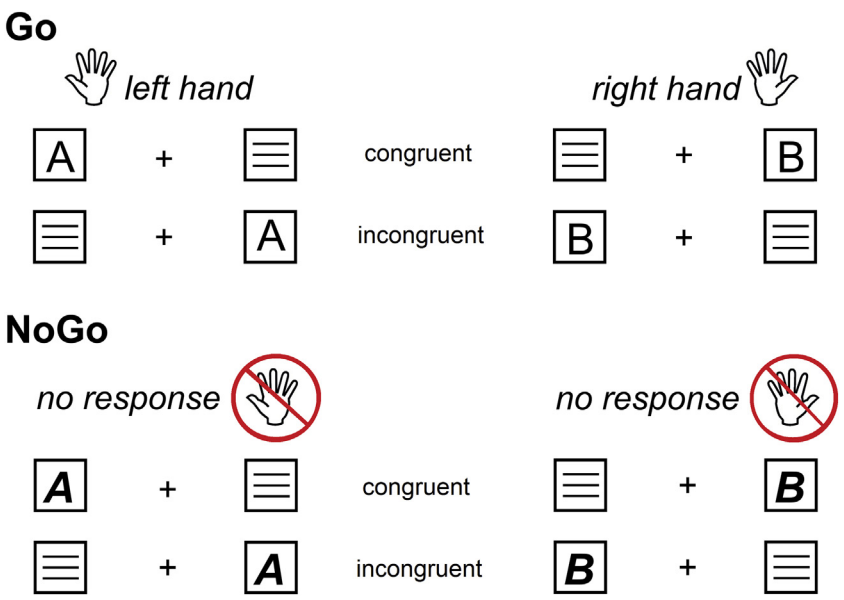

Fig. 1. The Simon Go/NoGo task with all stimulus configurations. "Go" stimuli are shown on the left site, "NoGo" stimuli are shown on the right side. The upper left panel shows stimuli "A" which require a left hand response. In the lower left panel stimuli "B" is presented, which require a response with the right hand. In addition, in the right panel stimuli "*A*" (upper panel) and "*B*" (lower panel) are shown, which both require no response (NoGo condition). "Congruent" and "incongruent" indicate the congruency between the side at which the stimulus is presented and the side of the response hand.

A fixation cross was always presented in the middle of screen and white stimuli were presented in white boxes on a black background. The boxes were presented on the left and right of the fixation cross (distance of 1.1° visual angle). Each trial began with the presentation of a letter (for 200 ms) in one of the boxes, which was either in normal font (i.e. 'A', 'B'), or in bold-italics (i.e. '*A*' or '*B*'). Letters in a normal font represented Go trials, letters in combined bold and italic font represented NoGo trials. For Go trials, and whenever an 'A' was displayed, a left hand response was required. A right hand response was required, whenever a 'B' was displayed. These responses were required regardless of the spatial position of the stimuli in the left or right box: In a congruent Go condition, stimuli were presented on the side of the hand carrying out the response. In the incongruent condition, stimuli were presented on the side opposite of the hand carrying out the response. This creates the Simon component of the task. Subjects were asked to respond within 250-1200 ms after stimulus presentation in Go trials. An incorrect response in that time-window was coded as error and if no response was obtained, trials were coded as misses. For NoGo trials, left side '*A*'s and right side '*B*'s, represented congruent NoGo trials, whereas left side '*B*'s and right side '*A*'s, represented incongruent NoGo trials. For NoGo trials, any response within 250-1200 ms after stimulus presentation represented a false alarm (i.e. a failure to inhibit the response). Each trial ended after 1700 ms. The inter-trial interval (ITI) was jittered between 1100 and 1600 ms. The experiment consisted of 720 trials [70% Go and 30% NoGo trials]. Fifty percent of these trials were congruent and 50% were incongruent (for more details on the task refer to (Chmielewski et al., 2018; Chmielewski and Beste, 2017)). The experiment was divided into six equally sized blocks with short breaks in between. It was ensured that all conditions were equally distributed across the blocks. Before the experiment, each subject was trained on the task using 40 trials.

2.3. EEG recording and analysis

The EEG was recorded and processed as done in a previous study on this task (Chmielewski et al., 2018) using 60 Ag/AgCl electrodes (500 Hz sampling rate; 'BrainAmp' amplifier, Brain Products Inc.). All electrode impedances were kept below 5 kΩ. The reference electrode was located at Fpz and the ground electrode was located at $\theta = 58$, $\phi = 78$. After recording, a band-pass filter from 0.5–20 Hz (48 dB/oct slope each) was applied and a raw data inspection was conducted to remove technical artifacts. Horizontal and vertical eye movements and pulse artifacts, were subsequently detected and corrected by means of independent component analysis (ICA; infomax algorithm). Then, cue-locked segments were formed: congruent Go trials, incongruent Go trials, congruent NoGo trials, and incongruent NoGo trials. Only trials with correct responses were included (i.e. no response on Nogo trials). The segments started 200 ms prior to the locking point and ended 2000 ms thereafter. An automated artifact rejection procedure was applied in the segmented data, with the following criteria: a maximal value difference above 200 μV in a 200 ms interval as well as an activity below 0.5 μV in a 100 ms period as rejection criteria. Overall, ~1.2% of trials were discarded. Then, a current source density (CSD) transformation was run, which eliminates the reference potential from the data and helps to find the electrodes showing the strongest effects (Nunez and Pilgreen, 1991). A baseline correction was performed in a time interval from −200 ms to 0 ms (i.e. stimulus presentation) before averaging.

To dissociate 'stimulus codes' from 'response selection codes' residue iteration decomposition (RIDE) was run using established protocols (Mückschel et al., 2017; Ouyang et al., 2011; Verleger et al., 2014). The RIDE toolbox is available on http://cns.hkbu.edu.hk/RIDE.htm. RIDE decomposes ERP components applying *L1*-norm minimization (i.e., obtaining median waveforms) and therefore minimizes residual error due to noise in the data (Ouyang et al., 2015a, 2015b). RIDE decomposes the ERP signal into clusters that correlated either to the stimulus onset (S-cluster) or to the response time (R-cluster), as well as a central C-cluster with variable latency, which is estimated initially and iteratively improved. The procedure used here is exactly the same as done in (Chmielewski et al., 2018) using the same experiment.

Since only infrequent responses are evident on NoGo trials, it is not possible to reliably estimate the R-cluster (Ouyang et al., 2013). Therefore, only the S-cluster and C-cluster are computed. Details on the algorithm to estimate the C-cluster can be found elsewhere (Ouyang et al., 2011, 2015a), Ouyang et al., 2013. During processing, the initial time window for the estimation of the C-cluster was set to 200 to 800 ms after stimulus onset. The time window is assumed to cover the range within which each component is supposed to occur (Ouyang et al., 2015b). The time window for the S-cluster was set to −200 to 400 ms around stimulus onset. For the RIDE cluster quantification, a visual inspection of the data was performed, which was also followed by a validation procedure using statistical methods (Mückschel et al., 2014). In detail, a validation procedure a following was applied: We defined a search interval (in which the component is expected to be maximal) for each ERP component. Next we applied CSD transformation of the data, because the CSD transformation has the effect of a

spatial filter that accentuates scalp topography (Nunez and Pilgreen, 1991). Subsequently afterwards we extracted the respective mean amplitudes at each of the 65 electrode positions and within each of the search intervals. Each electrode was compared against an average of all other electrodes using Bonferroni-correction for multiple comparisons (critical threshold, p = .0007). Only those, electrodes which showed significantly larger mean amplitudes (i.e., negative for N1 potentials and positive for P1 and P3 potentials) than the remaining electrodes were chosen.

Finally, this procedure revealed the same electrodes as previously been chosen on the basis of visual inspection of scalp topography plots.

In the S-Cluster the mean amplitude in the P1 time window was quantified in the time interval from 115 to 135 ms, and in the N1 time window in the time interval from 180 to 210 ms in Go and NoGo trials, at electrodes P7 and P8. At electrode FCz, data was quantified in the N2 time window between 315 and 345 ms. For the C-cluster it has already been shown that it reflects processes that are commonly reflected by the (NoGo)-P3 ERP- (Ouyang et al., 2017; Verleger et al., 2014; Wolff et al., 2017) but also by the N2 ERP-component (Chmielewski et al., 2018).

The C-cluster was quantified in Go and NoGo trials and revealed negative amplitudes at central electrodes (i.e. FC1 and Cz) between 310 and 350 ms and positive amplitudes at centro-parietal electrode sites (i.e. Pz) between 420 and 500 ms. C-cluster amplitudes were quantified at these electrodes and time windows. The statistical validation procedure confirmed this choice of electrodes and time windows.

For ERPs mean amplitude in the P1 time window was quantified in the time interval from 95 to 130 ms, and in the N1 time window in the time interval from 155 to 190 ms at electrodes P7 and P8. N2 mean amplitudes were quantified at electrode Cz in a time range from 290 to 335 ms. Finally P3 mean amplitudes were quantified at electrode Pz between ms. 350 and 400 ms.

2.4. Source localization

The source localization was based on the RIDE data, and the C-cluster in particular because only the C-cluster revealed differential effects. The analysis was performed using sLORETA (standardized low resolution brain electromagnetic tomography; (Pascual-Marqui, 2002), which provides a single linear solution to the inverse problem without localization bias (Marco-Pallarés et al., 2005; Pascual-Marqui, 2002; Sekihara et al., 2005). There is also evidence of EEG/(f)MRI and EEG/TMS studies underlining the validity of the sources estimated using sLORETA (Dippel and Beste, 2015; Sekihara et al., 2005). For sLORETA, the intracerebral volume is partitioned into 6239 voxels at 5 mm spatial resolution. The standardized current density at each voxel is calculated in a realistic head model using the MNI152 template. The OCD and the HC group were contrasted using statistical non-parametric mapping (SnPM) using the sLORETA-built-in voxel-wise randomization tests with 2000 permutations. Voxels with significant differences (p < .01, corrected for multiple comparisons) between contrasted conditions were located in the MNI-brain www.unizh.ch/keyinst/NewLORETA/sLORETA/sLORETA.htm

2.5. Statistics

The behavioral data were analyzed separately for Go and NoGo conditions using repeated measures ANOVA including the factor 'congruency' (congruent vs. incongruent) as within-subject factor and 'group' (OCD vs. HC) as between-subject factor. The neurophysiological data were analyzed using repeated measures ANOVAs including the factor 'condition' (Go vs. NoGo) and 'congruency' (congruent vs. incongruent) as within-subject factors and 'group' (OCD vs. HC) as between-subject factor. Greenhouse-Geisser correction was applied wherever it was necessary and all post-hoc tests were Bonferroni-corrected (all p < .05).

3. Results

3.1. Behavioral data

3.1.1. Go-Trials

The mixed effects ANOVA for the accuracy revealed a significant main effect of "congruency" ($F(1,53) = 10.56$, $p = .002$, $\eta_p^2 = 0.166$), indicating more hits in the congruent (91.71% ± 1.1) than in the incongruent condition (84.30% ± 2.8). Moreover, a significant main effect of "group" was observed ($F(1,53) = 6.87$, $p = .011$, $\eta_p^2 = 0.115$) showing more hits in HC (92.59% ± 2.5), compared to OCD patients (83.41% ± 2.45). The interaction "congruency x group" was not significant ($F(1,53) = 1.84$, $p = .181$). For the reaction time (RT) data, there was a significant main effect of "congruency" ($F(1,53) = 35.81$, $p < .001$, $\eta_p^2 = 0.408$), indicating shorter RTs in the congruent (587 ms ± 14) compared to the incongruent condition (613 ms ± 14). No further effects were evident (all $F < 3.06$, $p > .086$). Finally, the mixed effects ANOVA for misses in Go-trials revealed a significant main effect of "group" ($F(1,53) = 6.90$, $p = .011$, $\eta_p^2 = 0.115$), indicating significantly more misses in OCD (8.17% ± 1.67) vs HC (1.86% ± 1.72). No further effect was significant (all $F < 0.975$, $p > .328$).

3.1.2. NoGo-Trials

The rate of false alarms (FA, i.e. responses executed in NoGo trials) is the most important behavioral parameter in response inhibition paradigms and is shown in Fig. 2. The mixed effects ANOVA revealed a significant main effect of "congruency" ($F(1,53) = 23.12$, $p < .001$, $\eta_p^2 = 0.304$), with more FAs in congruent (17.38% ± 1.66), compared to incongruent trials (13.76% ± 1.69). Importantly, there was an interaction of "congruency x group" ($F(1,53) = 14.86$, $p < .001$, $\eta_p^2 = 0.219$). Post-hoc paired *t*-test revealed significantly more FAs in HCs (21.26% ± 2.94) compared to OCD patients (13.49% ± 1.6) during congruent trials ($t(40.15) = -2.32$, $p = .026$). No group differences were evident in incongruent trials ($t(53) = -0.58$, $p = .56$).

3.1.3. Neurophysiological data

The standard ERP-components (i.e. P1, N1, Nogo-N2 and Nogo-P3) are shown in the supplemental material including their statistical analysis. Briefly, none of these ERP-component reflected the hypothesized interaction "congruency x group" in NoGo trials, which was observed for the behavioral data ($F < 0.301$; $p > .586$). This is in line with the study hypotheses.

3.2. RIDE-decomposition

3.2.1. S-Cluster

The RIDE S-cluster data is shown in Fig. 3 including scalp topography plots. In line with previous studies (Chmielewski et al., 2018; Wolff et al., 2017), the S-Cluster was observed on occipital-temporal electrode sites (P7,P8) in the P1 and N1 time range and at electrode FCz in the N2 time range. However, neither in the P1 and N1 time range, nor in the N2 time range a significant main effect or interaction was observed (all $F < 3.48$, all $p > .067$). The same pattern was observed in a previous study on this tasks in adults (Chmielewski et al., 2018), showing that the combination of automatic and controlled processes during response inhibition seems not to be influenced by stimulus related processes.

3.2.2. C-Cluster

The RIDE C-cluster data is shown in Fig. 4 including scalp topography plots. The C-cluster showed both, negative amplitudes at fronto-central sites (FC1, Cz in the N2 time range) as well as positive amplitudes at parietal-central sites (Pz in the P3 time range), which is well in line with results from a previous study on the same paradigm (Chmielewski et al., 2018).

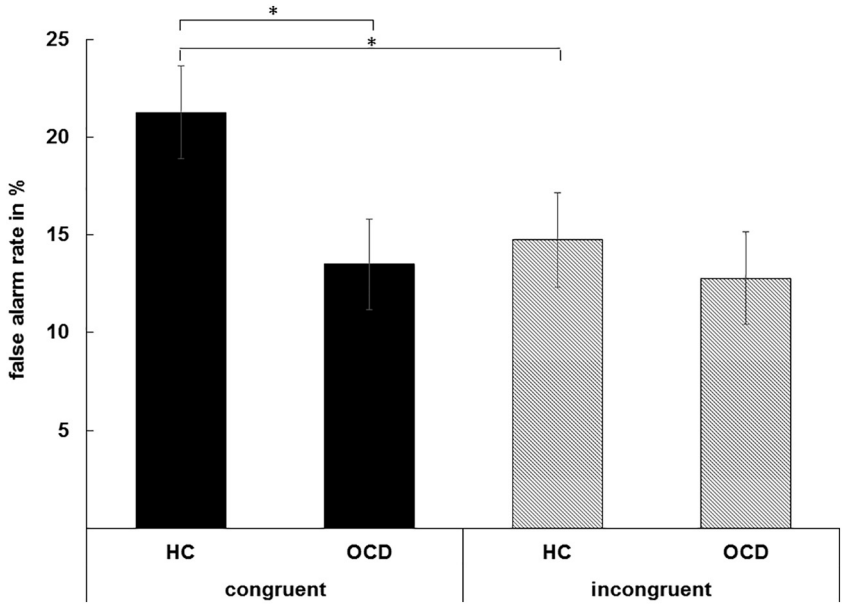

Fig. 2. Behavioral data showing the false alarm rate for congruent and incongruent NoGo trials. The mean and standard error of the mean (SE) are given. Asterisks show significant results on the $p < .05$ level.

In the N2 time window, the mixed effects ANOVA revealed a main effect of "electrode" ($F(1,53) = 6.83$, $p = .011$, $\eta_p^2 = 0.109$), showing increased (more negative) amplitudes at electrode Cz ($-16.29\,\mu V/m^2 \pm 1.62$) as compared to FC1 ($-12.93\,\mu V/m^2 \pm 1.47$). In addition a main effect of "condition" ($F(1,53) = 14.23$, $p < .001$, $\eta_p^2 = 0.203$) was found, showing more negative amplitudes during NoGo ($-16.33\,\mu V/m^2 \pm 1.62$) compared to Go trials ($-12.89\,\mu V/m^2 \pm 1.33$). Importantly, there was a three-way interaction of "congruency x condition x group" ($F(1,53) = 4.15$, $p = .046$, $\eta_p^2 = 0.069$). This effect corresponds to the interaction in NoGo trials observed in the behavioral data. In addition, C-cluster amplitudes in the congruent NoGo condition were significantly stronger (i.e. more negative) in the OCD group ($-19.73\,\mu V/m^2 \pm 3.60$) as compared to HCs ($-9.74\,\mu V/m^2 \pm 1.03$) ($t(32.29) = -2.12$, $p = .042$). The source localization using sLORETA show that modulations in the C-cluster in the N2 time window were associated with activation differences in the

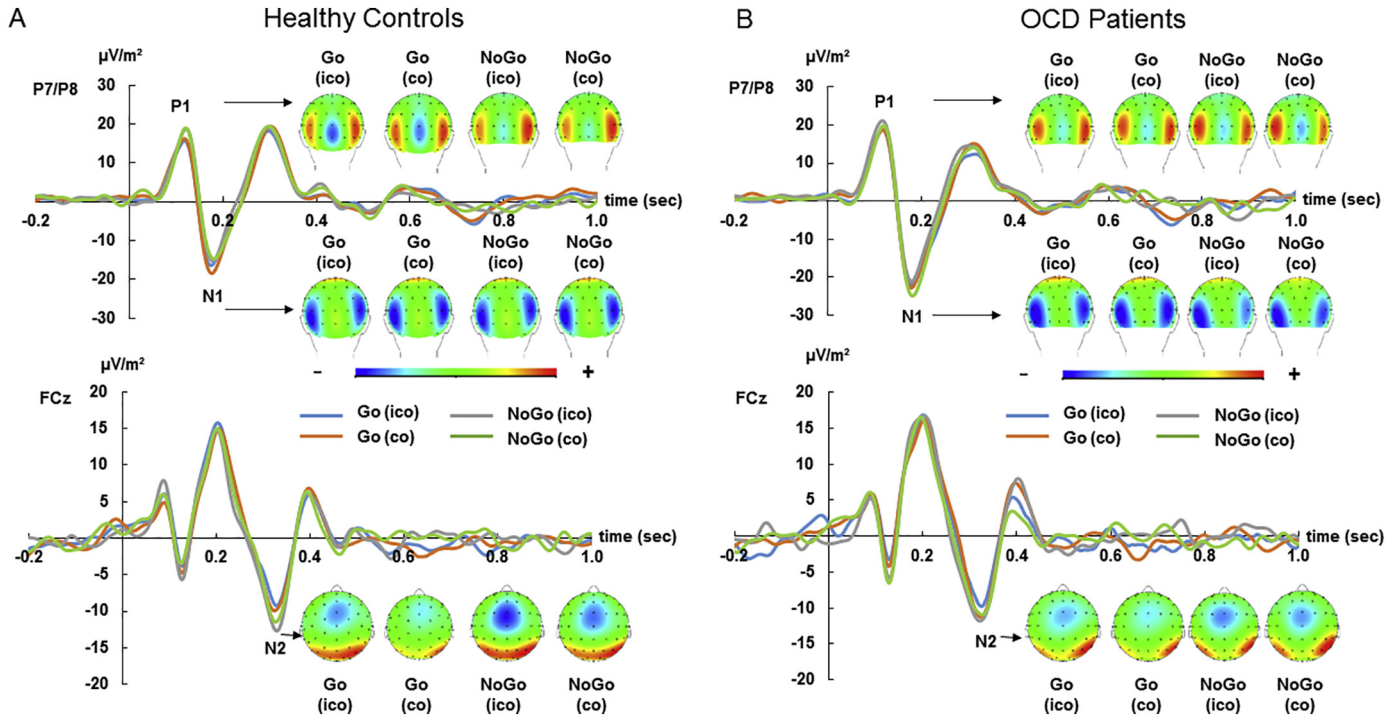

Fig. 3. (A) On the left side the S-Cluster is shown at electrodes P7, P8 and FCz for all experimental conditions, including the scalp topographies in HC. (B) On the right side the S-Cluster is shown at electrodes P7, P8 and FCz for all experimental conditions, including the scalp topographies in OCD patients. In both parts (A and B) the scalp topographies show the distribution of potentials at the peak of the S-Cluster at the shown electrodes/components (upper part P1 at pooled electrodes P7/P8; in the middle N1 at pooled electrodes P7/P8; lower part N2 at electrode FCz). In the topography plots, blue colors denote negativity and red colors denote positivity. The abbreviation "ico" means "incongruent", "co" means "congruent".

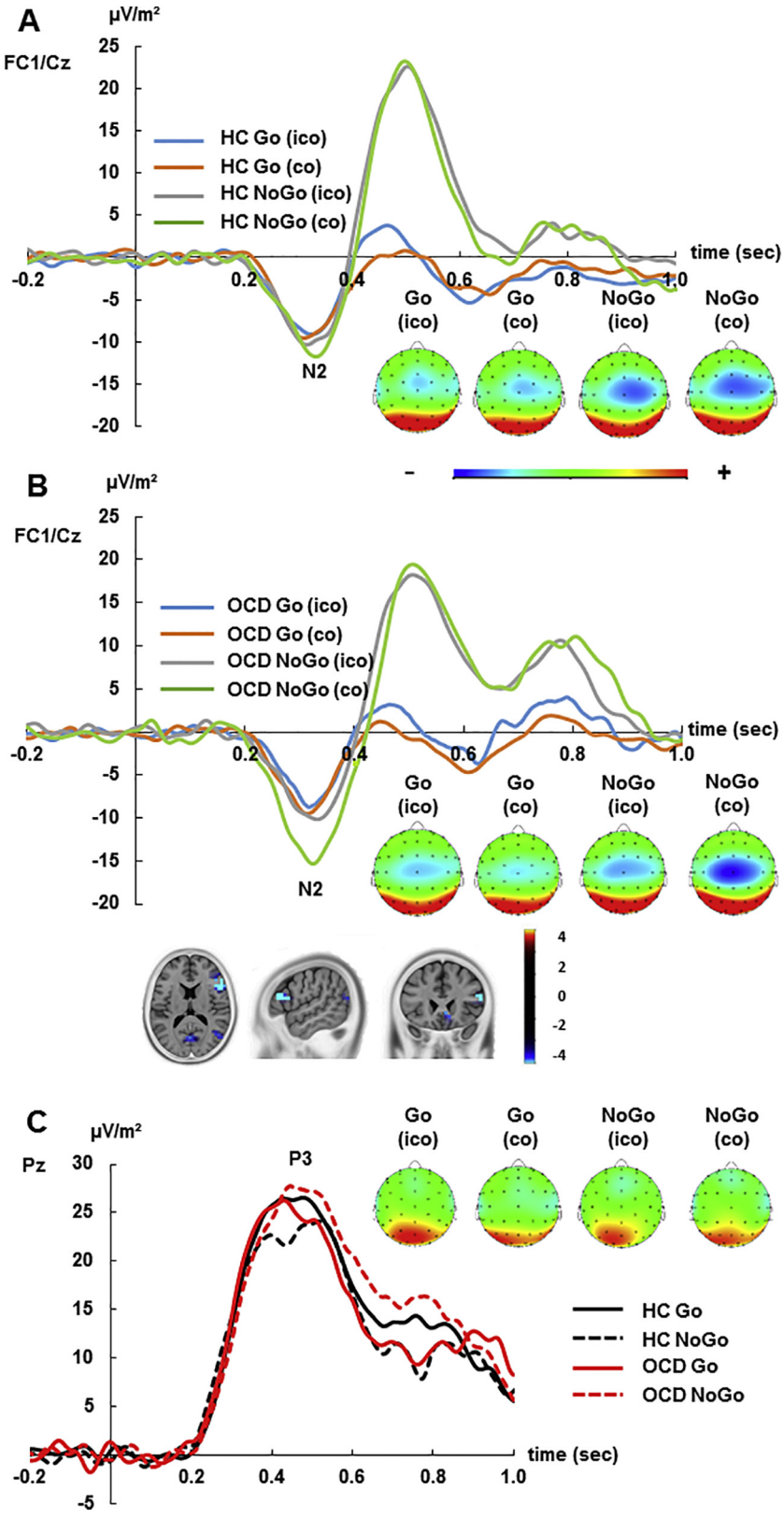

Fig. 4. (A) The C-Cluster is shown at pooled electrodes FC1 and Cz for all experimental conditions, including the scalp topographies in HC. (B) The C-Cluster is shown at pooled electrodes FC1 and Cz for all experimental conditions, including the scalp topographies in OCD patients. The sLORETA plots show a source in the right inferior frontal gyrus in the N2 time range comparing the congruent condition in NoGo trials between OCD patients and HC (corrected for multiple comparisons). (C) The C-Cluster is shown at electrode Pz for Go and NoGo trials, averaged for incongruent and congruent conditions, for HC and OCD patients. In all three parts (A, B and C) the scalp topographies show the distribution of potentials at the peak of the C-Cluster at the shown electrodes/components (part A and B: N2 at pooled electrodes FC1/Cz; part C: P3 at electrode Pz). In the topography plots, blue colors denote negativity and red colors denote positivity. The abbreviation "ico" = "incongruent", "co" = "congruent".

rIFG. C-cluster amplitudes in incongruent NoGo conditions did not show group differences ($t(29.69) = -1.12$, $p = .282$). In Go-conditions no group differences between congruent and incongruent trials was observed ($t(26) = 0.542$, $p = .593$). No further main effect or interaction was observed during N2-time range (all $F < 0.97$, $p > .328$).

For the positivity in the C-cluster at parietal electrode leads (shown in Fig. 4), the mixed effects ANOVA revealed a main effect of condition ($F(1,53) = 4.19$, $p = .046$, $\eta_p^2 = 0.075$) showing increased amplitudes during Go ($27.62\,\mu V/m^2 \pm 2.31$) as compared to NoGo trials ($25.53\,\mu V/m^2 \pm 2.47$), which is in line with previous research (Chmielewski et al., 2018). No further main effect or interaction was observed during P3 time range (all $F < 3.94$, $p > .052$).

4. Discussion

Research on response inhibition in OCD is dominated by the view of dysfunctional top-down cognitive control processes leading to dysfunctions to inhibit a pre-potent response (Berlin and Lee, 2018; Dalley et al., 2011). Yet, a currently neglected factor in research on response inhibition in OCD refers to the degree of automaticity which affects response inhibition performance (Dippel et al., 2015; Donkers and van Boxtel, 2004) and is needed to execute a pre-potent response. In fact, it has been shown that response inhibition depends on conjoint effects of automatic and controlled processes (Chmielewski et al., 2018; Chmielewski and Beste, 2017). In the current study we examined how conjoint effects of automatic and controlled processes are modulated in OCD. To this end, we examined a combined "Simon-Go/NoGo task". The false alarm data show that OCD patients committed less false alarms than HCs in the congruent Simon-NoGo condition, indicating better performance during congruent NoGo conditions as compared to HC. During the incongruent Simon-NoGo condition, OCD patients show less hits as compared to HC, possibly indicating stronger response tendencies during incongruent compared to congruent conditions in OCD. This observation seems to be in line with research of Kalanthroff et al. (2014), showing that changing the proportion of neutral versus congruent and incongruent trials in a conflict task favoring the neutral, produces faster RTs for neutral trials in OCD patients but not in controls. This may indicate that OCD patients remain alert even when less inhibitory control is needed. Importantly, however, the response speed was not different between OCD patients and HCs. In addition, no differential modulations of response accuracy in relation to the factor congruency were evident. This shows that the higher performance in OCD patients in the congruent NoGo condition is not an effect of a specific responding strategy and that there is no speed-accuracy tradeoff evident. Hence, OCD patients do not show the usual, healthy control-like deficits in response inhibition when processing is mediated via the "automatic" route. It seems that processing via the automated route is diminished in OCD, which leads to a paradoxical advantage in response inhibition in OCD patients, compared to HCs. A recent study examined ADHD patients using the same experimental procedure (Chmielewski et al., 2019). That study revealed that interference effects did not modulate response inhibition performance in ADHS patients (as opposed to healthy controls); i.e. there was an interaction of congruent and incongruent NoGo trials and group (ADHD patients vs. controls) (Chmielewski et al., 2019). Such an interaction was not evident in the current study. Therefore, OCD patients and ADHD patients seem to differ in how far they show an altered architecture of the response inhibition system.

For the current study, and on a neurophysiological level, the standard ERP data and the S-cluster data did not reveal differential effects between OCD patients and HCs. Such differential effects were observed for the C-cluster in the N2 time window. This is an expected finding, because previous results already suggested that 'response selection' codes (reflected by the C-cluster), but not 'stimulus codes' (reflected by the S-cluster) or a mixture of these processes (reflected by ERPs), best reflect conjoint modulations of "automatic" and "controlled" processes during response inhibition (Chmielewski et al., 2018). In particular, the C-cluster in the N2 time window was larger for OCD patients than HCs in the congruent NoGo condition. Thus, it seems that response selection processes are stronger in OCD patients in the congruent NoGo condition, compared to HCs. The sLORETA data show that these modulations in the C-cluster were associated with activation differences in the right inferior frontal gyrus (rIFG). This increase in response selection mechanisms in congruent NoGo trials may explain the observed paradoxical performance advantage in OCD patients in that condition. The rIFG is known to play a central role in inhibitory control processes (Aron et al., 2004, 2015; Garavan et al., 2006; Kelly et al., 2004; Konishi et al., 1998), and has been suggested to mediate a 'braking function' (Aron et al., 2014, 2015; Gillies and Willshaw, 1998). This behavioral brake has been suggested to be switched on when it is necessary to inhibit an action (Aron et al., 2014; Bianco et al., 2017). For compatible Simon trials, the dual process account states that response selection is driven by more automated processes (De Jong et al., 1994). Therefore, response inhibition is usually found to be more error-prone, when the processing is dominated by the automatic route (Chmielewski et al., 2018; Chmielewski and Beste, 2017). The fact that this is not the case in OCD patients suggests that braking processes 'become' more intensified than usual, when response selection is driven by the automatic route. This is evidenced by a higher C-cluster amplitude. The consequence is a relative benefit compared to HCs in response inhibition. Importantly, this paradoxical advantage can well be explained by known pathophysiological processes in OCD: Differences between processes associated with the unconditional (automatic) and the conditional (controlled) route response selection in Simon tasks strongly depend on striatal mechanisms (Dharmadhikari et al., 2015; Haag et al., 2015). Usually, striatal processes become more involved when response selection is driven by the controlled route (Dharmadhikari et al., 2015; Haag et al., 2015). This fits to theoretical concepts stating that striatal GABAergic medium spiny neurons (MSNs) play an important role during the controlled selection of responses (Bar-Gad et al., 2003; Redgrave et al., 1999; Redgrave and Gurney, 2006). Strong activity of the striatal MSN network increases response selection efficiency and performance during response inhibition. In line with that, higher striatal GABAergic concentrations are correlated with better response inhibition performance and the modulation of EEG-correlates during response inhibition (Quetscher et al., 2015). Interestingly, data suggest that OCD is associated with an increased activity of GABAergic MSNs, which do also not show a specific modulation of this hyperactivity by cortical projections (Burguiere et al., 2015; Burguière et al., 2013). This lack of a specific modulation of striatal hyperactivity in OCD patients may explain the results: Unlike HCs, striatal response selection mechanisms may even become involved in OCD patients when processes are dominated by the unconditional (automatic) route. Since OCD patients are then involving intensified striatal response selection mechanisms in a condition where this is likely not the case in HCs, a performance advantage emerges. Thus, the observed performance advantage is possibly the result of an otherwise pathological striatal hyperactivity and loss of a situation-specific modulation of response selection mechanisms in OCD (Burguiere et al., 2015; Burguière et al., 2013). Since HCs mainly involve striatal response selection mechanisms during the conditional ("controlled") selection of the appropriate response (Dharmadhikari et al., 2015; Haag et al., 2015) it seems reasonable that OCD patients and HCs did not differ in performance and neurophysiological parameters during incongruent NoGo trials. The finding that specifically C-cluster modulations associated with inferior frontal structures reflect the behavioral advantage of OCD patients corroborates the above explanation of the findings based on aberrant activity in neural circuits important for response selection mechanisms. This is because the C-cluster has been shown to specifically reflect response selection processes (Bluschke et al., 2017; Mückschel et al., 2017; Ouyang et al., 2017; Verleger et al., 2014, 2017; Wolff et al., 2017) for which fronto-striatal structures play an important role (Bar-Gad et al., 2003; Redgrave et al., 1999; Redgrave and Gurney, 2006). Moreover, above-mentioned 'braking functions' associated with the rIFG during response inhibition have also been suggested to emerge due to projections from the rIFG to subcortical (striatal) structures (Gillies and Willshaw, 1998).

Studies observed that OCD goes along with deviant intrinsic functional connectivity between brain networks and that moreover, alterations in the interaction between fronto-parietal network (FPN) and the default network (DMN) may contribute to aspects of the OCD phenotype (Kang et al., 2013; Stern et al., 2012). It was suggested that patients' inability to disengage from internally-generated thoughts may be explained by alterations in these networks. However, we observed increased performance in OCD patients and suggested that this

advantage is possibly the result of an otherwise pathological striatal hyperactivity and loss of a situation-specific modulation of response selection mechanisms in OCD (Burguiere et al., 2015; Burguière et al., 2013). The current results cannot be directly related to findings on fMRI resting state networks, since resting state data was not examined. This may be subject to future studies. In this regard, it also needs to be stressed that the current study examined adolescent OCD patients. Most studies, however, focus on adult OCD. Results of these studies show deficits in response inhibition - independent of the age of OCD patients. However, as mentioned in the introduction none of these studies, focus on the differentiation of automatic vs. controlled processes of response inhibition. Thus, further research disentangling the effects of response inhibition across the development of OCD seems to be highly recommended in order to give answers to the question if this effect could be extrapolated to adult OCD. Future studies shall also investigate the effects of psychopharmacological treatments. Within our study, we investigated 27 OCD participants out of these 27 only two patients receive medication (Fluoxetine). Since the serotonergic system has been implicated in response inhibition processes (Bari and Robbins, 2013), it may be possible that also the architecture of inhibitory control is modulated.

In summary, the results show that there is no general response inhibition deficit in adolescent OCD. When considering conjoint effects of automatic and controlled processes during the inhibition of responses paradoxical response inhibition advantages can emerge in OCD. These advantages are likely due to intensified 'braking processes' mediated via specific cognitive neurophysiological mechanisms associated with right inferior frontal structures in situations in which HCs do not deploy these intensified processes. Although our interpretation needs further investigation as well as replication at present, we assume that the effects are likely a result of an otherwise pathological fronto-striatal hyperactivity and loss of a situation-specific modulation of response selection mechanisms in OCD.

Funding

This work was supported by a Grant from the Else Kröner Fresenius Stiftung 2017_A101 to N.W. and partly by Grant from the Deutsche Forschungsgemeinschaft (DFB)0SFB 940 to V.R. and C.B.

Conflicts of interests

NW, WC and JB declare no competing or potential conflicts of interest. V. Roessner has received payment for consulting and writing activities from Lilly, Novartis, and Shire Pharmaceuticals, lecture honoraria from Lilly, Novartis, Shire Pharmaceuticals, and Medice Pharma, and support for research from Shire and Novartis. He has carried out (and is currently carrying out) clinical trials in cooperation with the Novartis, Shire, and Otsuka companies. C. Beste has received payment for consulting from GlaxoSmithKline, Novartis, Genzyme and Teva.

Acknowledgements

We thank all participants.

Appendix A. Supplementary data

Supplementary data to this article can be found online at https://doi.org/10.1016/j.nicl.2019.101893.

References

Allen, C., Singh, K.D., Verbruggen, F., Chambers, C.D., 2018. Evidence for parallel activation of the pre-supplementary motor area and inferior frontal cortex during response inhibition: a combined MEG and TMS study. R. Soc. Open Sci. 5, 171369. https://doi.org/10.1098/rsos.171369.

Aron, A.R., 2007. The neural basis of inhibition in cognitive control. Neuroscientist 13, 214–228. https://doi.org/10.1177/1073858407299288.

Aron, A.R., Robbins, T.W., Poldrack, R.A., 2004. Inhibition and the right inferior frontal cortex. Trends Cogn. Sci. 8, 170–177. https://doi.org/10.1016/j.tics.2004.02.010.

Aron, A.R., Robbins, T.W., Poldrack, R.A., 2014. Inhibition and the right inferior frontal cortex: one decade on. Trends Cogn. Sci. 18, 177–185. https://doi.org/10.1016/j.tics.2013.12.003.

Aron, A.R., Cai, W., Badre, D., Robbins, T.W., 2015. Evidence supports specific braking function for inferior PFC. Trends Cogn. Sci. 19, 711–712. https://doi.org/10.1016/j.tics.2015.09.001.

Bar-Gad, I., Morris, G., Bergman, H., 2003. Information processing, dimensionality reduction and reinforcement learning in the basal ganglia. Prog. Neurobiol. 71, 439–473.

Bari, A., Robbins, T.W., 2013. Inhibition and impulsivity: behavioral and neural basis of response control. Prog. Neurobiol. 108, 44–79. https://doi.org/10.1016/j.pneurobio.2013.06.005.

Berlin, G.S., Lee, H.-J., 2018. Response inhibition and error-monitoring processes in individuals with obsessive-compulsive disorder. J. Obsessive-Compuls. Relat. Disord. 16, 21–27. https://doi.org/10.1016/j.jocrd.2017.11.001.

Bianco, V., Berchicci, M., Perri, R.L., Spinelli, D., Di Russo, F., 2017. The proactive self-control of actions: time-course of underlying brain activities. NeuroImage 156, 388–393. https://doi.org/10.1016/j.neuroimage.2017.05.043.

Bluschke, A., Chmielewski, W.X., Mückschel, M., Roessner, V., Beste, C., 2017. Neuronal intra-individual variability masks response selection differences between ADHD subtypes-a need to change perspectives. Front. Hum. Neurosci. 11, 329. https://doi.org/10.3389/fnhum.2017.00329.

Burguière, E., Monteiro, P., Feng, G., Graybiel, A.M., 2013. Optogenetic stimulation of lateral orbitofronto-striatal pathway suppresses compulsive behaviors. Science 340, 1243–1246.

Burguiere, E., Monteiro, P., Mallet, L., Feng, G., Graybiel, A.M., 2015. Striatal circuits, habits, and implications for obsessive–compulsive disorder. Curr. Opin. Neurobiol. 30, 59–65.

Chambers, C.D., Bellgrove, M.A., Gould, I.C., English, T., Garavan, H., McNaught, E., Kamke, M., Mattingley, J.B., 2007. Dissociable mechanisms of cognitive control in prefrontal and premotor cortex. J. Neurophysiol. 98, 3638–3647. https://doi.org/10.1152/jn.00685.2007.

Chmielewski, W.X., Beste, C., 2017. Testing interactive effects of automatic and conflict control processes during response inhibition–a system neurophysiological study. NeuroImage 146, 1149–1156.

Chmielewski, W.X., Mückschel, M., Beste, C., 2018. Response selection codes in neurophysiological data predict conjoint effects of controlled and automatic processes during response inhibition. Hum. Brain Mapp. 39, 1839–1849.

Chmielewski, W., Bluschke, A., Bodmer, B., Wolff, N., Roessner, V., Beste, C., 2019. Evidence for an altered architecture and a hierarchical modulation of inhibitory control processes in ADHD. Dev. Cogn. Neurosci. 36, 100623. https://doi.org/10.1016/j.dcn.2019.100623.

Dalley, J.W., Everitt, B.J., Robbins, T.W., 2011. Impulsivity, compulsivity, and top-down cognitive control. Neuron 69, 680–694.

De Jong, R., Liang, C.C., Lauber, E., 1994. Conditional and unconditional automaticity: a dual-process model of effects of spatial stimulus-response correspondence. J. Exp. Psychol. Hum. Percept. Perform. 20, 731–750.

Dharmadhikari, S., Ma, R., Yeh, C.-L., Stock, A.-K., Snyder, S., Zauber, S.E., Dydak, U., Beste, C., 2015. Striatal and thalamic GABA level concentrations play differential roles for the modulation of response selection processes by proprioceptive information. Neuroimage 120, 36–42.

Di Russo, F., Lucci, G., Sulpizio, V., Berchicci, M., Spinelli, D., Pitzalis, S., Galati, G., 2016. Spatiotemporal brain mapping during preparation, perception, and action. NeuroImage 126, 1–14. https://doi.org/10.1016/j.neuroimage.2015.11.036.

Dippel, G., Beste, C., 2015. A causal role of the right inferior frontal cortex in the strategies of multi-component behaviour. Nat. Commun. https://doi.org/10.1038/ncomms7587.

Dippel, G., Chmielewski, W., Mückschel, M., Beste, C., 2015. Response mode-dependent differences in neurofunctional networks during response inhibition: an EEG-beamforming study. Brain Struct. Funct. 1–11. https://doi.org/10.1007/s00429-015-1148-y.

Donkers, F.C.L., van Boxtel, G.J.M., 2004. The N2 in go/no-go tasks reflects conflict monitoring not response inhibition. Brain Cogn. Neurocogn. Mech. Perform. Monitr. Inhibit. Control 56, 165–176. https://doi.org/10.1016/j.bandc.2004.04.005.

Döpfner, M., Görtz-Dorten, A., Lehmkuhl, G., 2008. Diagnostik-System für Sychische Störungen im Kindes-und Jugendalter nach ICD-10 und DSM-IV. Huber, Bern.

Foa, E.B., Huppert, J.D., Leiberg, S., Langner, R., Kichic, R., Hajcak, G., Salkovskis, P.M., 2002. The obsessive-compulsive inventory: development and validation of a short version. Psychol. Assess. 14, 485–496.

Folstein, J.R., Van Petten, C., 2008. Influence of cognitive control and mismatch on the N2 component of the ERP: a review. Psychophysiology 45, 152–170. https://doi.org/10.1111/j.1469-8986.2007.00602.x.

Garavan, H., Hester, R., Murphy, K., Fassbender, C., Kelly, C., 2006. Individual differences in the functional neuroanatomy of inhibitory control. Brain Res. Cont. Attent. Act. 1105, 130–142. https://doi.org/10.1016/j.brainres.2006.03.029.

Gillies, A.J., Willshaw, D.J., 1998. A massively connected subthalamic nucleus leads to the generation of widespread pulses. Proc. R. Soc. Lond. B Biol. Sci. 265, 2101–2109. https://doi.org/10.1098/rspb.1998.0546.

Goletz, H., Döpfner, M., 2011. ZWIK, Zwangsinventar für Kinder und Jugendliche, in: Klinisch-Psychiatrische Ratingskalen Für Das Kindes- Und Jugendalter. Hogrefe, Göttingen, pp. 489–493.

Haag, L., Quetscher, C., Dharmadhikari, S., Dydak, U., Schmidt-Wilcke, T., Beste, C., 2015. Interrelation of resting state functional connectivity, striatal GABA levels, and cognitive control processes. Hum. Brain Mapp. 36, 4383–4393. https://doi.org/10.1002/hbm.22920.

Hommel, B., 2011. The Simon effect as tool and heuristic. Acta Psychol. 136, 189–202. https://doi.org/10.1016/j.actpsy.2010.04.011.

Huster, R.J., Plis, S.M., Calhoun, V.D., 2015. Group-level component analyses of EEG: validation and evaluation. Front. Neurosci. 9, 254. https://doi.org/10.3389/fnins.2015.00254.

Kalanthroff, E., Anholt, G.E., Henik, A., 2014. Always on guard: test of high vs. low control conditions in obsessive-compulsive disorder patients. Psychiatry Res. 219, 322–328. https://doi.org/10.1016/j.psychres.2014.05.050.

Kang, D.-H., Jang, J.H., Han, J.Y., Kim, J.-H., Jung, W.H., Choi, J.-S., Choi, C.-H., Kwon, J.S., 2013. Neural correlates of altered response inhibition and dysfunctional connectivity at rest in obsessive–compulsive disorder. Prog. Neuro-Psychopharmacol. Biol. Psychiatry 40, 340–346.

Kelly, A.M.C., Hester, R., Murphy, K., Javitt, D.C., Foxe, J.J., Garavan, H., 2004. Prefrontal-subcortical dissociations underlying inhibitory control revealed by event-related fMRI. Eur. J. Neurosci. 19, 3105–3112. https://doi.org/10.1111/j.0953-816X.2004.03429.x.

Keye, D., Wilhelm, O., Oberauer, K., Stürmer, B., 2013. Individual differences in response conflict adaptations. Front. Psychol. 4, 947. https://doi.org/10.3389/fpsyg.2013.00947.

Konishi, S., Nakajima, K., Uchida, I., Sekihara, K., Miyashita, Y., 1998. No-go dominant brain activity in human inferior prefrontal cortex revealed by functional magnetic resonance imaging. Eur. J. Neurosci. 10, 1209–1213. https://doi.org/10.1046/j.1460-9568.1998.00167.x.

Kornblum, S., Hasbroucq, T., Osman, A., 1990. Dimensional overlap: cognitive basis for stimulus-response compatibility–a model and taxonomy. Psychol. Rev. 97, 253–270.

Lehnen, K., Pietrowsky, R., 2015. Inhibition deficit in OCD patients. J. Behav. Ther. Exp. Psychiatry 47, 60–67.

Marco-Pallarés, J., Grau, C., Ruffini, G., 2005. Combined ICA-LORETA analysis of mismatch negativity. NeuroImage 25, 471–477. https://doi.org/10.1016/j.neuroimage.2004.11.028.

Mückschel, M., Stock, A.-K., Beste, C., 2014. Psychophysiological mechanisms of interindividual differences in goal activation modes during action cascading. Cereb. Cortex N. Y. N 1991 (24), 2120–2129. https://doi.org/10.1093/cercor/bht066.

Mückschel, M., Stock, A.-K., Dippel, G., Chmielewski, W., Beste, C., 2016. Interacting sources of interference during sensorimotor integration processes. NeuroImage 125, 342–349. https://doi.org/10.1016/j.neuroimage.2015.09.075.

Mückschel, M., Chmielewski, W., Ziemssen, T., Beste, C., 2017. The norepinephrine system shows information-content specific properties during cognitive control – evidence from EEG and pupillary responses. NeuroImage 149, 44–52. https://doi.org/10.1016/j.neuroimage.2017.01.036.

Nunez, P.L., Pilgreen, K.L., 1991. The spline-Laplacian in clinical neurophysiology: a method to improve EEG spatial resolution. J. Clin. Neurophysiol. Off. Publ. Am. Electroencephalogr. Soc. 8, 397–413.

Nunez, P.L., Srinivasan, R., Westdorp, A.F., Wijesinghe, R.S., Tucker, D.M., Silberstein, R.B., Cadusch, P.J., 1997. EEG coherency. I: statistics, reference electrode, volume conduction, Laplacians, cortical imaging, and interpretation at multiple scales. Electroencephalogr. Clin. Neurophysiol. 103, 499–515.

Ouyang, G., Herzmann, G., Zhou, C., Sommer, W., 2011. Residue iteration decomposition (RIDE): a new method to separate ERP components on the basis of latency variability in single trials. Psychophysiology 48, 1631–1647. https://doi.org/10.1111/j.1469-8986.2011.01269.x.

Ouyang, G., Schacht, A., Zhou, C., Sommer, W., 2013. Overcoming limitations of the ERP method with R esidue I teration D ecomposition (RIDE): A demonstration in go/no-go experiments. Psychophysiology 50 (3), 253–265.

Ouyang, G., Sommer, W., Zhou, C., 2015a. A toolbox for residue iteration decomposition (RIDE)–a method for the decomposition, reconstruction, and single trial analysis of event related potentials. J. Neurosci. Methods 250, 7–21. https://doi.org/10.1016/j.jneumeth.2014.10.009.

Ouyang, G., Sommer, W., Zhou, C., 2015b. Updating and validating a new framework for restoring and analyzing latency-variable ERP components from single trials with residue iteration decomposition (RIDE). Psychophysiology 52, 839–856. https://doi.org/10.1111/psyp.12411.

Ouyang, G., Hildebrandt, A., Sommer, W., Zhou, C., 2017. Exploiting the intra-subject latency variability from single-trial event-related potentials in the P3 time range: a review and comparative evaluation of methods. Neurosci. Biobehav. Rev. 75, 1–21. https://doi.org/10.1016/j.neubiorev.2017.01.023.

Pascual-Marqui, R.D., 2002. Standardized low-resolution brain electromagnetic tomography (sLORETA): technical details. Methods Find. Exp. Clin. Pharmacol. 24 (Suppl D), 5–12.

Petermann, F., Petermann, U., 2010. Hamburg-Wechsler-Intelligenztest für KinderIV (HAWIK-IV), 3rd ed. Huber, Bern.

Quetscher, C., Yildiz, A., Dharmadhikari, S., Glaubitz, B., Schmidt-Wilcke, T., Dydak, U., Beste, C., 2015. Striatal GABA-MRS predicts response inhibition performance and its cortical electrophysiological correlates. Brain Struct. Funct. 220, 3555–3564. https://doi.org/10.1007/s00429-014-0873-y.

Redgrave, P., Gurney, K., 2006. The short-latency dopamine signal: a role in discovering novel actions? Nat. Rev. Neurosci. 7, 967.

Redgrave, P., Prescott, T.J., Gurney, K., 1999. The basal ganglia: a vertebrate solution to the selection problem? Neuroscience 89, 1009–1023.

Ridderinkhof, K.R., 2002. Micro- and macro-adjustments of task set: activation and suppression in conflict tasks. Psychol. Res. 66, 312–323. https://doi.org/10.1007/s00426-002-0104-7.

Ridderinkhof, K.R., Ullsperger, M., Crone, E.A., Nieuwenhuis, S., 2004a. The role of the medial frontal cortex in cognitive control. Science 306, 443–447. https://doi.org/10.1126/science.1100301.

Ridderinkhof, K.R., van den Wildenberg, W.P.M., Segalowitz, S.J., Carter, C.S., 2004b. Neurocognitive mechanisms of cognitive control: the role of prefrontal cortex in action selection, response inhibition, performance monitoring, and reward-based learning. Brain Cogn. 56, 129–140. https://doi.org/10.1016/j.bandc.2004.09.016.

Sekihara, K., Sahani, M., Nagarajan, S.S., 2005. Localization bias and spatial resolution of adaptive and non-adaptive spatial filters for MEG source reconstruction. NeuroImage 25, 1056–1067. https://doi.org/10.1016/j.neuroimage.2004.11.051.

Stern, E.R., Fitzgerald, K.D., Welsh, R.C., Abelson, J.L., Taylor, S.F., 2012. Resting-state functional connectivity between fronto-parietal and default mode networks in obsessive-compulsive disorder. PLoS ONE 7, e36356.

Stock, A.-K., Gohil, K., Huster, R.J., Beste, C., 2017. On the effects of multimodal information integration in multitasking. Sci. Rep. 7, 4927. https://doi.org/10.1038/s41598-017-04828-w.

van Velzen, L.S., Vriend, C., de Wit, S.J., van den Heuvel, O.A., 2014. Response inhibition and interference control in obsessive–compulsive spectrum disorders. Front. Hum. Neurosci. 8, 419.

Verleger, R., Metzner, M.F., Ouyang, G., Śmigasiewicz, K., Zhou, C., 2014. Testing the stimulus-to-response bridging function of the oddball-P3 by delayed response signals and residue iteration decomposition (RIDE). NeuroImage 100, 271–280. https://doi.org/10.1016/j.neuroimage.2014.06.036.

Verleger, R., Siller, B., Ouyang, G., Śmigasiewicz, K., 2017. Effects on P3 of spreading targets and response prompts apart. Biol. Psychol. 126, 1–11. https://doi.org/10.1016/j.biopsycho.2017.03.011.

Wolff, N., Mückschel, M., Beste, C., 2017. Neural mechanisms and functional neuroanatomical networks during memory and cue-based task switching as revealed by residue iteration decomposition (RIDE) based source localization. Brain Struct. Funct. https://doi.org/10.1007/s00429-017-1437-8.

Wylie, S.A., Ridderinkhof, K.R., Bashore, T.R., van den Wildenberg, W.P.M., 2010. The effect of Parkinson's disease on the dynamics of on-line and proactive cognitive control during action selection. J. Cogn. Neurosci. 22, 2058–2073. https://doi.org/10.1162/jocn.2009.21326.